

Reduce Defects by Controlling the Spraying Process via Images Compare and Revamping Lean Six Sigma Toolbox

Abed AM*

Ideal-Standard Egypt Spray section, Zagazig University, Egypt

Abstract

Ideal-Standard factory suffers from disturbance in covering them Bathtubs by chemical liquid, which must cover all surfaces the same thickness. The main reason for that suffering is the emergence of bubbles in the liquid via vortex phenomenon (i.e., waste) that cause a defect in spraying process. This phenomenon is one of the hydrodynamic instability that pushes the liquid in the hoses with different pressures, then unbalance covers' layer of spraying liquid on a Bathtubs and reduce its resists against heating circumstances. The Vortex flow is subject to a number of major structural changes involving very large disturbances when a characteristic ratio of catalyst to axial velocity components is varied. Therefore, this paper proposed a VSCM algorithm (vortex stream control map) that discusses via DMIAC roadmap through two phases. The first describes and detect the waste by imaging and monitoring the vortex and comparing them with standard saving in local database. The second use the Genetic code to select the best camera position and manipulating the database that used in decision making through control step to cessation spraying process if the bubbles move out of its allowable range.

Keywords: Six-sigma; Vortex position control; Circulation number; Reynolds number; Image verification

Introduction

The term "vortex bursting" is used to denote the abrupt disorganization of a slender vortex that occurs when a characteristic ratio of catalyst to axial velocity components is varied. The defining features of the phenomenon include the very pronounced deceleration of the stream flow along the axis of the vortex accompanied by radial divergence of the stream surfaces [1]. The waste is every phenomenon leads to defect. This paper discusses DMIAC roadmap through two phases. The first describes and detect the waste (i.e., vortex and bubbles) through two sequential steps; the first determine the position via imaging and monitoring it; and the second use DOE to control the significant factors reduce this phenomena. The second phase use the Genetic code to select the best camera's path line and manipulating the database (i.e.; comparing between the standard case and the moment of the vortex generating and determine its type; then back to step 2 in phase one) that used in decision making through control step to cessation spraying process if the bubbles move out of its allowable range. Surveillance via imaging revealed that there are three distinct types of the vortex based on Reynolds number (Re) and circulation number (Ω) of the flow were varied. The kinetic range was found to be dependent on both Re and Ω of the flow. Whereas; for all Re values any increase in Ω always results in moving the vortex position upstream (defect case). The vortex position values are smaller for anti-clockwise flow direction than that; when vanes were set at clockwise flow direction for long and short hose. The Factory performance remains unpredictable in spite of the considerable literature on manufacturing productivity improvement; and the long history of manufacturing as there is no widespread agreement on how best be performed. Productivity measurement and improvement goes hand in hand; because one cannot improve what one cannot measure. To ensure successfully implementation of eliminating defects; a Vortex Stream Control Map (VSCM) algorithm is used; which is a combination between C# code and mechanical system based on monitoring the kinetic vortex range. The lean six sigma methodology will present a good recommend to eliminate this waste by continuously measure for DOE outputs; based on the cause and effect [2]; which initiating the VSCM to revamp its toolbox.

In 2015, the case study factory analyze its performance that shows a potential requirements to improve the process efficiency to reduce both time; costs and add more processes control. So; the reasons that effect on efficiency must be controlled to increase utilization of resources especially operators [3]. This work uses the DMAIC procedures that collect lean and six-sigma phases to describe a VSCM that used to control processes; which must be improved to match the new lean six-sigma; DMIAC ([Define; Measure; Imaging; Analysis] phase 1 and [Control] phase 2) [4].

There is characteristically; an appreciable axial compound of motion in addition to the swirl; or catalyst component. Such a vortex core is readily set up by passing a fluid through a pipe and imparting swirl with a set of vanes at entry. The phenomenon is of crucial significance in several devices of technological importance; such as delta wings (aircraft); Peckham and Atkinson [5]; Srigrarom and Rizwan [6]; Srigrarom and Lewpiriyawong [7]; draft tube of hydraulic turbines; Sharma et al. [8]; and Cervants [9] and swirling combustors; Stein and Kempf [10] and Tangermann and Pfitzner [11]. Aksel and kaya [12] and Jochmann [13] gave numerical computations of the vortex breakdown phenomenon taking place in a cylinder.

Main objective

The factory aim to increase its productivity between 8%:10%; leading to an equivalent savings in standard hours which will impact the factory indices (E1:95% to; E2:99%); with monetary saving value of L.E 95; 835.31/year. The VSCM is shown in Figure 1; which illustrates the sequential phases of vortex stream control map through DMIAC roadmap.

*Corresponding author: Abed AM, Ideal-Standard Egypt Spray section, Zagazig University, Egypt, Tel: +201008118736; E-mail: leansixsigmazero defect@gmail.com

Received January 09, 2017; Accepted January 28, 2017; Published January 31, 2017

Citation: Abed AM (2017) Reduce Defects by Controlling the Spraying Process via Images Compare and Revamping Lean Six Sigma Toolbox. Ind Eng Manage 6: 205. doi:10.4172/2169-0316.1000205

Copyright: © 2017 Abed AM. This is an open-access article distributed under the terms of the Creative Commons Attribution License, which permits unrestricted use, distribution, and reproduction in any medium, provided the original author and source are credited.

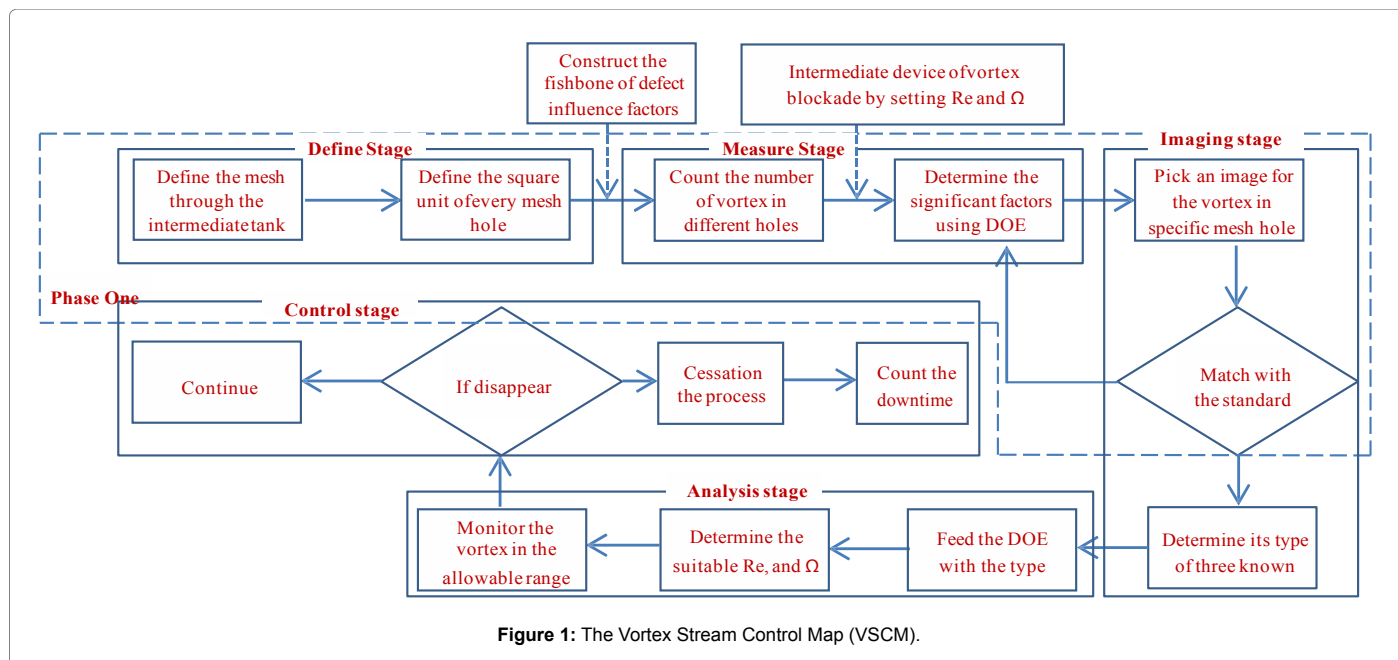


Figure 1: The Vortex Stream Control Map (VSCM).

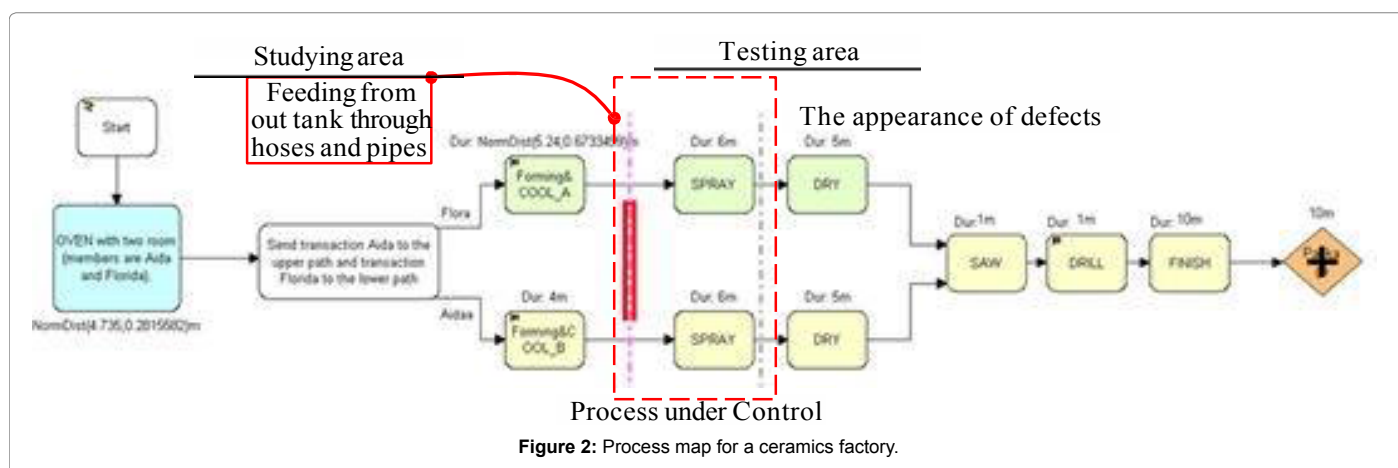


Figure 2: Process map for a ceramics factory.

Define Stage

This stage based on extensive experimental; numerical and theoretical research; the vortex position which depends on its shape remains controversial and no generally accepted explanation has emerged. The aim of the present investigation is to determine the mesh dimension dependence of the vortex core modes and its position on the Reynolds number (Re) and circulation number (Ω) in a vertical cylindrical feeding intermediate pipe with constant diameter and length of ($L=60$ cm) as well as for clockwise and anti- clockwise flow direction using dye injection. The process map is a sequential pictorial for the processes executed in the factory; (Figure 2) being designed by I-Grafx software. This figure illustrates the precedence processes required to produce bathtubs.

The factory produces bathtubs through seven sequential stages (thermoforming; forming and cooling; spraying; drying via heating; trimming; drilling; and finishing); with various in productivity. The next phases focus to determine the reasons which affect productivity and have a relation with inputs/Req.

The problem is defined and data collected to feed Mini-Tab software. All subsequent figures are outputs depending on these data (Figure 3).

Measure Stage

The measurement stage applied on the collected data from the shop-floor (Figures 2 and 3). The Pareto chart shows in Figure 4 discusses all causes affecting on the production line efficiency and cause downtime for more than 18000 sec/week. Therefore; the proposed VSCM add more control on transactions executed in the shop floor to reduce the stoppage times.

Device description

To verify these requirements and test the effected factors; a special test device has been designed and constructed in fluid mechanics via U.S.C.C experience house in 10th of Ramadan city. A schematic diagram of the test device is given in Figure 5; which illustrates the fourteen components used in our experiment.

The constant head supply tank is composed of two coaxial circular

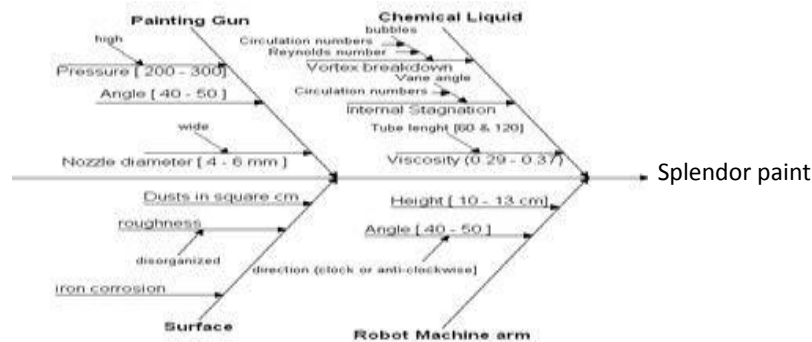


Figure 3: Cause and effect of painting Ibeam bathtubs model.

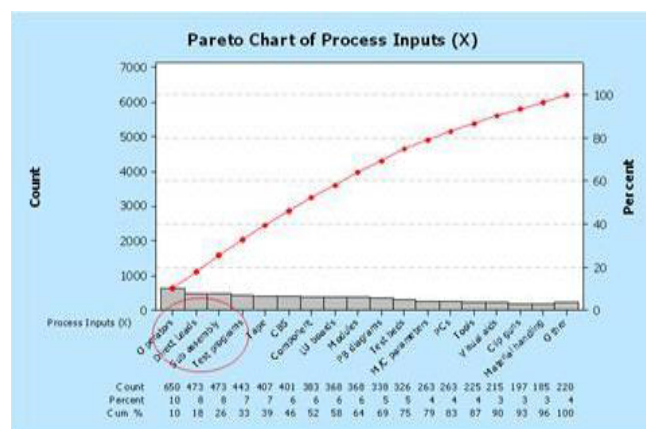


Figure 4: Pareto chart for process inputs.

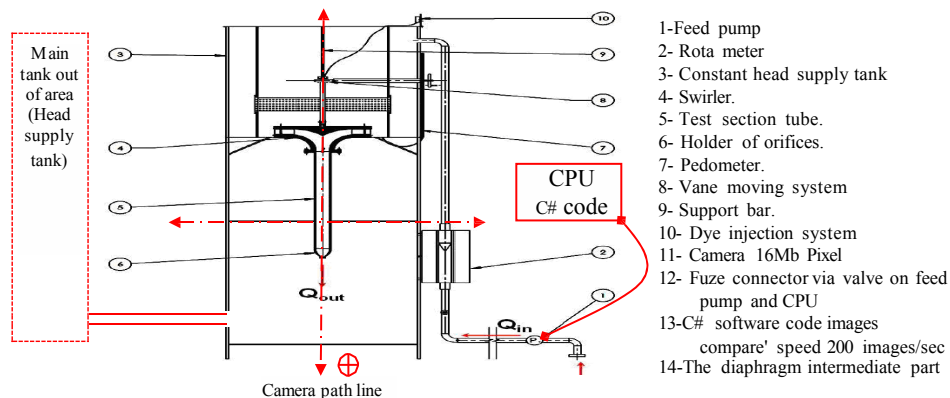


Figure 5: Prototype device used in controlling system experimentally.

cross section tanks. The experimental model tank (mediator) is constructed from two stages; the bottom part have three sides made of transparent acrylic sheet 0.12 cm thickness to facilitate visualization of the vane angle setting and have equilateral dimensions of 60 cm and 40 cm height. The above part with equilateral dimensions of 60 cm and 28 cm height located coaxially with the bottom tank. The diaphragm between the bottom and above part has 200 holes; of 0.12 cm diameter; located on a height of 50 cm from lower end. These holes are distributed in rows and are covered by a very narrow plastic mesh in order to have a calm flow at the swirled entrance.

These vanes were placed symmetrically in a circular array around

the center body at a radius of 15 cm. Since the amount of swirl imparted on the fluid is affected by the vane angle setting Φ so it was necessary to design a precise system for the movement and changing the vane angles.

To determine the downstream effect on the vortex phenomena; two pipe of lengths 60 and 120 cm were used. The two pipes have constant inner diameter of 3 cm. The tube was mounted vertically and fixed with the lower plate of the swirled through two flanges. The lower end of the tube was equipped with an orifice holder. The set of 15 orifices; were used orifice bore diameter ranged from 0.15 cm to 1 cm in order to alter corresponding to Reynolds numbers ranged from 662 to 9935 for short

tube and from 872 to 10737 for long tube. A scale was stuck on the outer surface of the tube to measure breakdown position.

This paper based on measuring the effect of varying Reynolds and circulation numbers on the vortex breakdown position as well as on the swirl angle distribution in a zone ahead of breakdown. The circulation number Ω was varied by changing the vane angle setting through a swirled for clockwise and anti-clockwise flow directions as illustrated in Figure 6 while the Reynolds number was changed by controlled inlet valve opening and by using a group of orifices which were fitted at the downstream end of the pipe test section Leibovich [14]. All these factors tabulated in Table 1 these levels were fed to Minitab and appeared the importance of set nozzle diameter and must study the best Reynolds number and Circulation number as shown in Figure 7 and Table 1.

Image Stage (Imaging the Vortex Breakdown Modes)

This stage focuses on imaging the vortex and bubbles and save it in database to use it in comparing process later. The database classified based on the above data to three fields; every one concentrates on bubbles mode will be debated as follows:

Image 1 - wide spiral mode

The central dye traveled along the pipe test section axis with no deflection when the vanes directed radially $\Phi=0$. As the swirl was

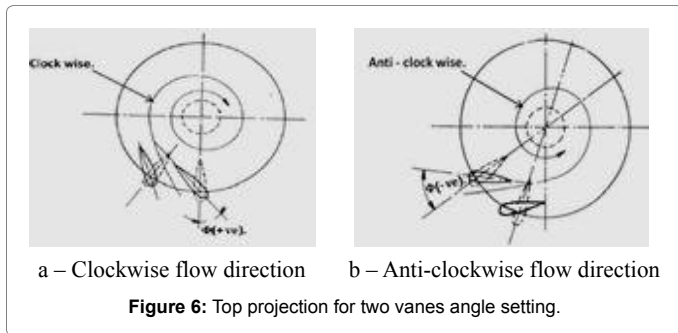


Figure 6: Top projection for two vanes angle setting.

	spraying Angle	Pressure	Robot arm angle	Reynolds number	Circulation number	Nozzle diameter	Viscosity
Low	40°	200 Pascal	40°	662	1.176	4 mm	0.29
High	50°	300 Pascal	50°	3312	1.286	6 mm	0.37

Spraying angle	Pressure	Robot arm angle	Reynolds number	Circulation number	Nozzle diameter	Defect Bathtubs
05	055	05	660	171.6	4	16
45	055	05	0010	170.6	4	01
05	055	45	660	171.6	6	04
05	055	45	660	170.6	4	1.
05	055	45	660	171.6	6	06
05	055	05	0010	171.6	4	14
45	055	05	0010	170.6	6	61
05	055	45	0010	170.6	6	0.
45	055	45	660	171.6	6	00
05	055	45	0010	171.6	4	10
05	055	05	660	170.6	6	06
45	055	45	0010	170.6	4	0.
45	055	05	0010	171.6	6	4.
45	055	05	660	171.6	4	0
05	055	05	0010	171.6	6	4.

Table 1: The influence factors used in DOE for spraying process.

imparted gradually to the fluid the central dye filament shows a slight oscillation in the filament near the downstream end of the tube test section. As the swirl was increased further the central filament moved gently; but distinctly; off axis at a nearly constant azimuth location in height between (42.5% to 48.2%) of total tank height.

According to the observations obtained during the experiments; it appears that a wide spiral mode is dominated between Re 1946: 2615 and same Ω 1.286 that shown in Map-I (Figure 8.1a and 8.1b). Whereas Figure 8.2 shows the helix case at Re 1520 and Ω 1.996. If we couldn't assassinating this vortex will create flattened bubbles.

Image 2 - flattened bubble mode

The flattened bubble occasionally evolved directly form Map-I. This transformation either occurred spontaneously; at fixed flow condition; or could be induced by slight increase of the swirl. In both

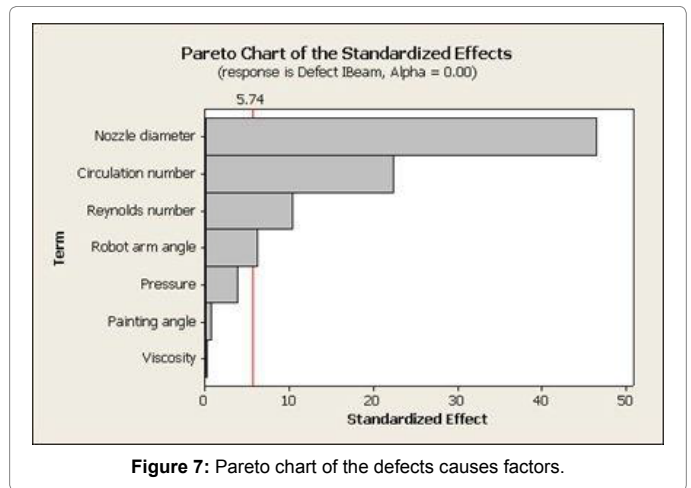


Figure 7: Pareto chart of the defects causes factors.

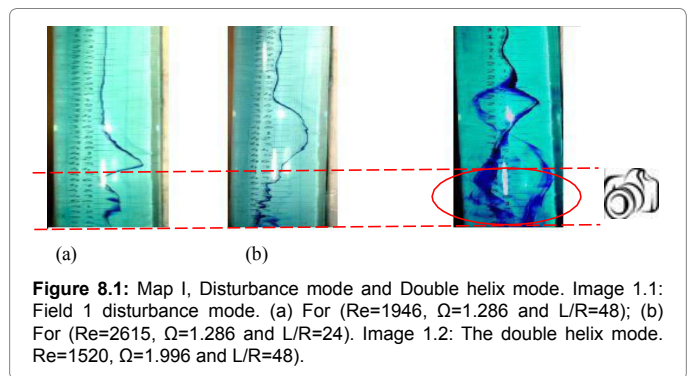


Figure 8.1: Map I, Disturbance mode and Double helix mode. Image 1.1: Field 1 disturbance mode. (a) For (Re=1946, $\Omega=1.286$ and $L/R=48$); (b) For (Re=2615, $\Omega=1.286$ and $L/R=24$). Image 1.2: The double helix mode. Re=1520, $\Omega=1.996$ and $L/R=48$.

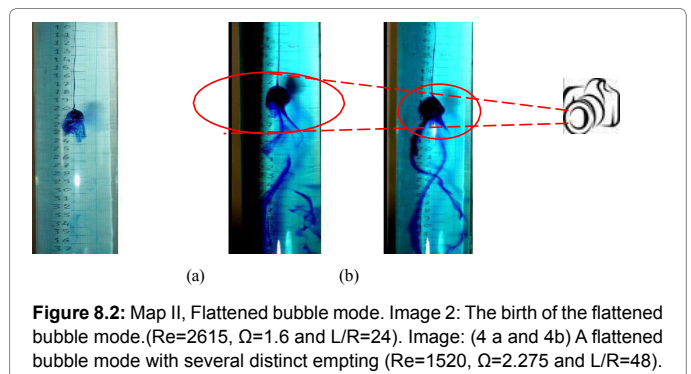


Figure 8.2: Map II, Flattened bubble mode. Image 2: The birth of the flattened bubble mode.(Re=2615, $\Omega=1.6$ and $L/R=24$). Image: (4 a and 4b) A flattened bubble mode with several distinct emptying (Re=1520, $\Omega=2.275$ and $L/R=48$).

cases; the sheared deflected and began to roll up; back toward the initial point of deflection; into a tight spiral. As this occurred; the filament downstream totally disappeared; including that all the dye reaching the disturbance has been recirculated; (Figure 8.2). After few seconds the dye began to exit from this recirculation zone and travel downstream; and the flattened bubble disturbance was fully formed. Usually; the dye leaves the recirculation zone in a fairly random fashion; occasionally; several distinct emptying paths were formed; as shown in Figure 8.2(4a and 4b).

Axisymmetric bubble mode

This case is known as the axisymmetric case of vortex breakdown. The bubble form is characterized by stagnation point on the swirl axis far from the bottom by 12%:16.012% of the total height of the tank; followed by an abrupt expansion of the centerline dye filament to form the envelope of a bubble of the recirculating fluid.

The envelope has high degree of the axis symmetric over most of its length; but the rear is not closed and is asymmetric as show in Figure 8.3(5). After a distance of approximately one bubble length; the new core deflected; following an abrupt kink; into a loose spiral configuration. This spiral seldom formed another bubble; which is possibly due to the instabilities; and after a few turns broke into large scale turbulence.

In fact; the bubble was observed to fill and empty in two different ways. In the first way; as shown in Figure 8.3(6.1) for $Re=1787$ and $\Omega=2.48$; the bubble was filled and emptied at diametrically opposite location near the rear bubble end; i.e.; at any instant the bubble was being filled at one azimuthal location and was being emptied at another azimuthal location; 180 degree away from the first. The downstream end of the breakdown was tilted; and the filling took place at that point farthest upstream and the emptying occurred near the farthest downstream point. The emptying tail of the breakdown tended to the return to the tube axis; (Figure 8.3(6.2)) for $Re=3312$ and $\Omega=1.996$. This case of filling and emptying was the most commonly observed one.

The second way is shown in Figure 8.3(6.3); for $Re=2535$ and $\Omega=2.275$; which was rarely observed; when the bubble has the temporary an appearance of dye on the axis inside it. The filament took the form of a screw worm and extended from just downstream of the nose of bubble to the downstream end of the bubble before being broken up. This filament was fed by a reservoir of dye located near the nose of the bubble. The screw worm filament would then appear and persist until the reservoir was exhausted.

The previous figures indicate that lack of controlling is the most severe effect on production. Sub- assembly stoppages occur frequently with progressive effect on production rate.

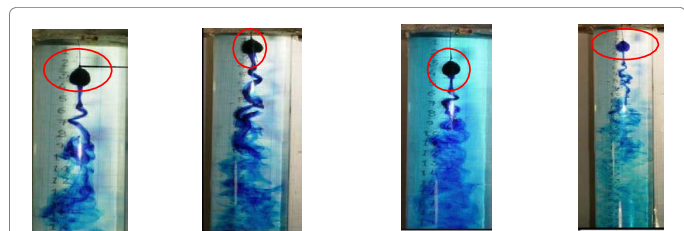


Figure 8.3: Map III, Axisymmetric Flattened bubble mode. Image 5: The axisymmetric vortex breakdown mode ($Re=2615$, $\Omega=2.275$, $L/R=24$). Image 6.1: The wake instability for filling and emptying of the bubble. ($Re=1787$, $\Omega=2.48$ and $L/R=24$). Image 6.2: The emptying tail of the breakdown tended to return to the tube axis. ($Re=3312$, $\Omega=1.996$ and $L/R=24$). Image 6.3: The spiralling of the vortex core in the bubble. ($Re=2535$, $\Omega=2.275$ and $L/R=24$).

Analysis Phase

This stage consumes six months and based on GA to determine the imaging position; the total stoppage time illustrated in Figure 9 was 1632 min to week 17; and this stoppage occurred due to shortage in feeding received from the supplier tank because of pressure variation due to bubbles. Depending on the Reynolds number based on the tube diameter; Re ; and the intensity of the swirling motion; the vortex core immediately downstream of the breakdown region is known to undergo remarkable transformations; which in most cases; are characterized by unsteady; three dimensional fluctuations; Sarpkaya [15,16]; Faler and Leibovich [17]; Garg and Leibovich [18]; Leibovich [14]; and Lucca-Negro and O' Doherty [19].

Experimental calculation via genetic code

If database can manipulate 11000 images/min to compare with standard saved. In this experiment three modes were observed; two of these modes are classified as wide spiral (repeated 4000 times/shift and tackle 3000 of them) and flattened bubbles (repeated 400 times/shift and tackle 280). The other mode is the so-called bubble axis-symmetric (repeated 100 times/shift and tackle 50). Figure 10 illustrates that there is no significant interaction between significant factors; Figure 11 illustrates

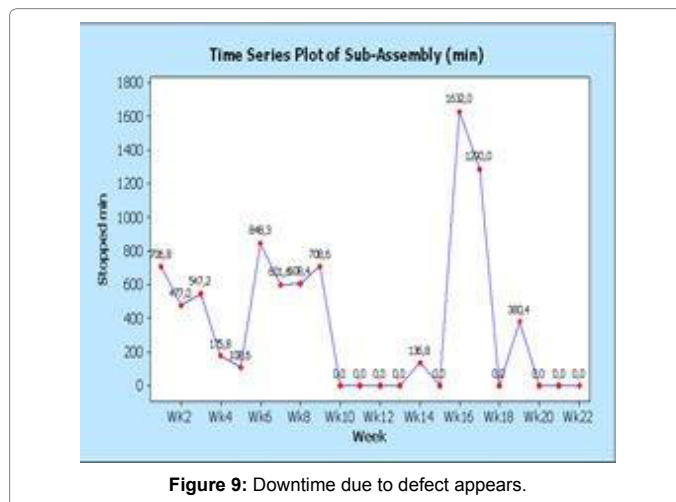


Figure 9: Downtime due to defect appears.

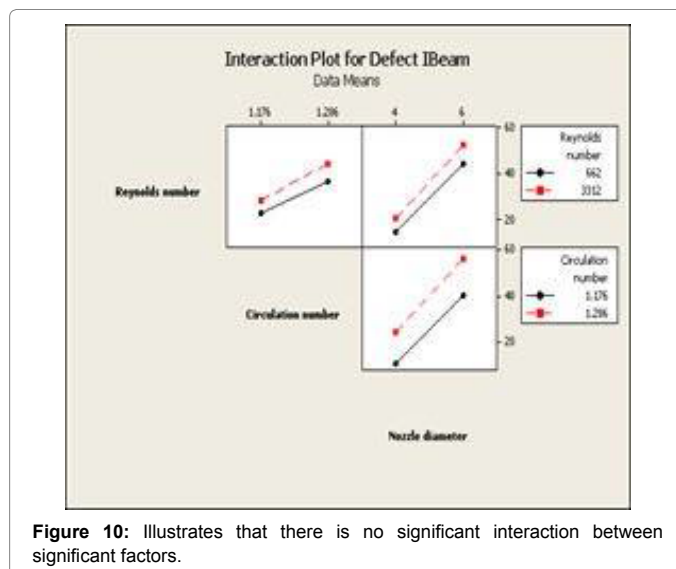


Figure 10: Illustrates that there is no significant interaction between significant factors.

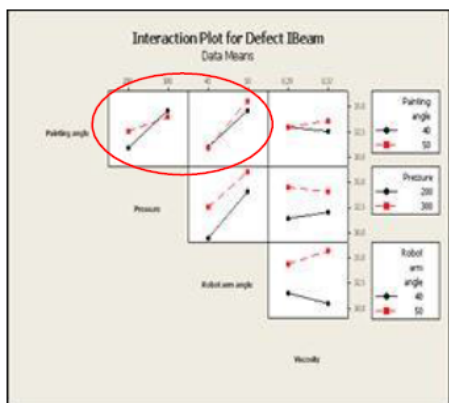


Figure 11: The interaction between other factors.

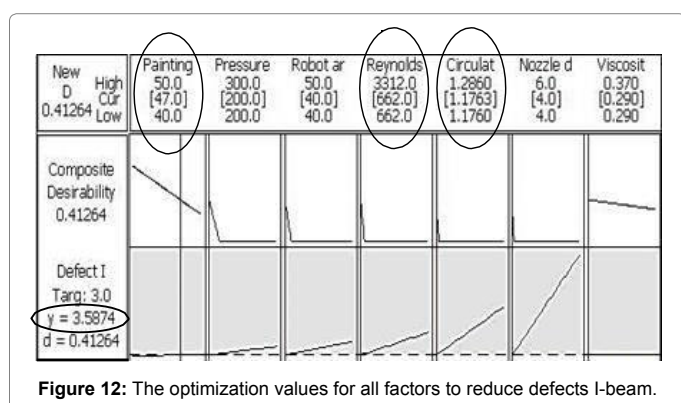


Figure 12: The optimization values for all factors to reduce defects I-beam.

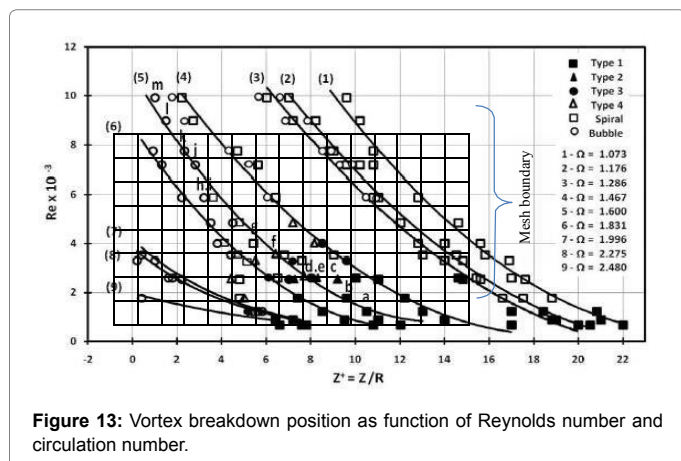


Figure 13: Vortex breakdown position as function of Reynolds number and circulation number.

the interaction between spraying angle with pressure and robot arm angle; and finally Figure 12 illustrates the optimization values for all factors to reduce defects Bathtubs to 3.4 ppm. The experimental study was conducted for pipe 60 cm long ($L/R=24$). The set of Experiments were performed under constant Reynolds number; Re ; while the circulation number; Ω ; was increased and significant. The vanes angles equal spraying angle multiply robot arm angle was found range covered in the experiments from 40° to 50° and Figure 13 illustrate that effective setup is 47° whereas the corresponding circulation range from 1.073 to 2.48 and the effective setup is 1.1763; respectively. For each vane angle setting the flow pattern was observed and the types as well as the axial position of the flow disturbance were recorded [20-25].

The population=50; the generations=30; the crossover rate=60%; and the bit length=4. This data required to predict the probability of cam position along the intermediate tank.

Control Stage

Vortex position results

The vortex position is the distance from the pipe entrance to the point at which the vortex is bursting. This bursting was showed to move upstream and downstream in an unpredictable way with no noticeable change in the external conditions. The vortex position is regarded as the average value of the minimum and the maximum movement of the vortex bubble [26,27]. As mentioned before the present experiments were carried out with the two swirl flow directions; and applied on the two pipe with dimensionless; $L/R=24$.

The circulation numbers for both pipe cases were ranged from 1.073 to 2.48 in the clockwise flow direction and from 1.073 to 1.831 in the anti-clockwise flow direction. The Reynolds number was adjusted in both directions to 662 for $L/R=24$.

Results of vortex position with $L/R=24$: The results of the dimensionless vortex position normalized by tube radius; $Z^+=Z/R$; for pipe $L/R=24$ are plotted against Re for six different values of Ω at clockwise flow direction in “Figure 13”. It can be seen from this figure that; the type and the disturbance location are dependent on both the Re and Ω . For fixed flow rate the disturbance mode is moved upstream as the imparted swirl was increased. For fixed circulation number (Ω) the disturbance was also moved upstream as Reynolds number (Re) was increased. Figure 13 illustrate at $\Omega=1.6$ and $Re=1241$ the disturbance was found to be wide spiral (Figure 8.1) at a distance about $Z^+=10.5$; point (a). When Reynolds number is increased to 1787 the Figure 8.1 is still being occurred but the disturbance moved upward to a new position of $Z^+=9.6$ point (b).

Controlling system

This section focuses on camera position to reduce the alarm time of tackling the waste. The next nested analysis sheet of probability for bubbles appears in restricted square area 12% to 48.2% from bottom of tank.

The fitness value of consuming time where r is the # of bubbles $1.7+3.4r$; the output is time in min. if the population in this case 20; mating chromosomes 10; mutation rate 0.2 and generations 0.25 [28-30].

Conclusion

Some of interesting conclusions can be drawn from implementing VSCM that helps in tackling the main reasons of spraying process failing; which is a waste (e.g.; vortex and bubbles):

- 1) The results revealed that there are a total of three distinct shapes of the vortex core as Re and Ω of the flow were varied. Two of these shapes (wide spiral) and (flattened bubble) occurred at Re 662 to 2615 for $L/R=24$. The other shapes appears at the highest values of Re and defined by bubble (axis-symmetric)
- 2) The bubble case occasionally occurred at the flow condition in the hysteresis zone and the bubble case become dominant and shrank in size (both diameter and length) as the Re or Ω was increased.
- 3) The vortex position was found to be dependent on both Re and Ω of the flow. whereas; for all Re values an increase in Ω always results in moving the vortex position upstream.

4) A considerable increase in Ω leads to a transformation to other shapes. An upstream movement of the breakdown is also resulted; in general; when Re is increased of a constant value circulation number Ω .

5) The vortex position values are smaller for anti-clockwise flow direction than that; when vanes were set clockwise flow direction short tube ($L/R=24$).

6) In state of circulation number equal to 1.176 a small influence of the vortex position values can be noted for long and short pipe with clockwise and anti-clockwise flow direction.

7) In case of clockwise flow direction the dead position occur downstream in the short pipe than that in long pipe at circulation number $\Omega=1.286$; but when circulation number increased up to 1.6 the dead vortex position occurs early in the short tube than that in the long tube.

8) In case of anti-clockwise flow direction the dead vortex position always happened downstream in the short pipe than that in the long pipe for all circulation numbers except when circulation number equal or greater than 1.600; a very small effect on the dead vortex position can be noticed.

Acknowledgements

I wish to express my deep indebtedness and sincere gratitude for the invaluable advices; and scientific spirit support of Editorial Board; during the publication this paper.

References

1. Peckham DH, Atkinson SA (1957) Preliminary results of low speed wind tunnel tests on a gothic wing of aspect ratio. 1.0. ARC technical report, CP No.50.
2. Sarpkaya T (1971) On stationary and travelling vortex breakdown. *J Fluid Mech* 45: 545-559.
3. Hall MG (1972) Vortex breakdown. *Rev of Fluid Mech* 4: 195-218.
4. Leibovich, Ann S (1978) The structure of vortex breakdown. *Rev of Fluid Mech* 10: 221-246.
5. Faler JH, Leibovich S (1977) Disrupted states of vortex flow and vortex breakdown. *J Phys Fluid* 20: 1385-1400.
6. Garg AK, Leibovich S (1979) Spectral characteristics of vortex breakdown flow field. *J Phys Fluid* 22: 2053-2064.
7. Leibovich S (1984) Vortex stability and breakdown: survey and extension. *AIAA Journal* 22: 1192-1206.
8. Aksel MH, Kaya MT (1992) A numerical simulation of the axisymmetric vortex breakdown in a tube. *Applied Mathematical Modeling* 16: 414-422.
9. Sarpkaya T (1995) Turbulent vortex breakdown. *J Phys Fluid* 7: 2301-2303.
10. Jochmann P, Sinigersky A, Hehel M (1996) Numerical simulation of a processing vortex breakdown. *International J. of Heat and Fluid Flow* 27: 192-203.
11. Sharma CL, Soundranayagam, Somkrishan S, Mukund TS (1998) Dependence of vortex breakdown on angular momentum parameter in draft tube flows. *Current Science* 75: 1355-1363.
12. Lucca-Negro O, O'Doherty T (2001) Vortex breakdown: a review. *Pro Energy combustion Sci* 27: 431-481.
13. Mata TM (2001) Life cycle assessment of different reuse percentages for glass beer bottles. *International Journal of Life Cycle Assessment* 6: 58-63.
14. Baggaley M (2004) *Practical Lean Accounting*. Productivity Press, New York, NY. p: 359.
15. Harvey JK (2006) Analysis of the vortex breakdown phenomenon. Imperial Collage, Department of aeronautics 14: 585-592.
16. Stein O, Kempf A (2007) LES of the Sydney swirl flame series: A steady of vortex breakdown in isothermal and reacting flows. *Proceeding of the Combustion Ins* 3: 11755-1763.
17. Srigrarom S, Ridzwan M (2007) An experimental investigation of perturbations on vortex breakdown over delta wings. 16th Australasian fluid mechanics conference, Crown Plaza, Gold Coast, Australia.
18. Srigrarom S, Lewpiriyawong N (2007) Controlled vortex breakdown on modified Delta Wings. *J of Visualization* 10: 299-307.
19. Cervants MJ (2009) Counter rotating runner cone in a Kaplan elbow draft tube for increased efficiency. 3rd IAHR International meeting of the workgroup on cavitation and dynamic problems in hydraulic machinery and systems, Brno, Czech Republic.
20. Tangermann E, Pfitzner M (2009) Evaluation of combustion models for combustion-induced vortex breakdown. *Journal of Turbulence*.
21. Richard Szeliski (2010) *Computer Vision: Algorithms and Applications*. Springer Science & Business Media. pp: 10-16.
22. Walshe K, Harvey G, Pauline J (2010) *Connecting Knowledge and Performance in Public Services: From Knowing to Doing*. Cambridge University Press. p: 175.
23. Davidson G (2011) *Waste Management Practices: Literature Review*.
24. Ries E (2011) *The Lean Startup: How Today's Entrepreneurs Use Continuous Innovation to Create Radically Successful Businesses*. Crown Business 978-0307887894.
25. Kanade T (2012) *Three-Dimensional Machine Vision*. Springer Science & Business Media. ISBN 978-1-4613-1981-8.
26. Wilschut LI, Addink EA, Heesterbeek JAP, Dubyanskiy VM, Davis SA, et al. (2013) Mapping the distribution of the main host for plague in a complex landscape in Kazakhstan: An object-based approach using SPOT-5 XS, Landsat 7 ETM+, SRTM and multiple Random Forests. *International Journal of Applied Earth Observation and Geoinformation* 23: 81-94.
27. Huffington Post (2015) Human waste may be flush with gold, silver, and other valuable metals.
28. Barghout L (2014) Visual Taxometric Approach to Image Segmentation Using Fuzzy-Spatial Taxon Cut Yields Contextually Relevant Regions. *Information Processing and Management of Uncertainty in Knowledge-Based Systems*. Springer International Publishing 443: 163-173.
29. Abed AM, Samir Farag Control Vortex Position in Vertical Tube to Reduce Spray Defects and Revamping Six-Sigma Image Verification Tool. *The Egyptian Int J of Eng Sci and Technology* 17: 178-185.
30. Shingo K (2010) High-speed vision systems and projectors for real-time perception of the world. *IEEE Computer Society Conference on Computer Vision and Pattern Recognition-Workshops*. 2010: 100-107.